A 300-J Multigigawatt CO_2 Laser

MARTIN C. RICHARDSON, A. J. ALCOCK, KURT LEOPOLD, AND PETER BURTYN

Abstract—**The development of a new transverse electric discharge scheme has permitted the excitation of large volumes of CO_2, N_2, and He mixtures with beam cross sections up to 60 cm² in area. The scheme utilizes as a preionizer a sheet of small arc discharges produced prior to the main discharge and situated behind a perforated anode. Time-resolved photography establishes that rapid volumetric ionization of the gas between the electrodes occurs concurrent with the formation of these arcs. This behavior is consistent with a preionization mechanism depending upon UV photoexcitation of the gas. A parametric study has shown that reproducible discharge conditions in 30 percent CO_2 gas mixtures are obtained with input energies of >300 J·l⁻¹, resulting in energy extraction efficiencies of ~10 percent and an average small-signal gain of ~4.3 percent cm⁻¹. The laser is modular in construction and, when a number of discharge modules are employed in series in a simple oscillator configuration, energies of ~300 J with peak powers of several gigawatts are obtained.**

I. Introduction

PROGRESS in the development of high-power high-energy gas lasers has been marked by several significant advances in recent years. These were initially stimulated by the application of high-voltage pulses to longitudinally excited CO_2 laser systems [1], which resulted in many orders of magnitude improvement in power and energy capabilities [2], and lately in the generation of pulses of megawatt power and several hundred joules energy [3]. This method of excitation permits operation at pressures of several tens of torr without the occurrence of avalanche breakdown in the gaseous medium. However, by incorporating high-voltage electric excitation transverse to the beam axis [4], operation at total gas pressures approaching [5] or equal to [6] atmospheric pressure was demonstrated. The advent of such transverse excitation at atmosphere pressure (TEA) lasers made possible the construction of relatively simple devices capable of producing pulsed megawatt power outputs with gain, unit volume energy storage, and conversion efficiencies considerably greater than had hitherto been achieved. However, the development of high-energy CO_2 laser systems with powers in the gigawatt range demands the arc-free excitation of large volumes of gas mixtures with beam cross sections sufficiently large that the radiation power density within the laser gas remains below the optical breakdown threshold of the medium. Various excitation schemes have been developed toward this aim and considerable success has been achieved with several methods of transverse excitation of the gas medium. So-called "double-discharge" lasers [5], [7]–[12], which rely upon the production of a thin electron gas layer in close proximity to a mesh, wire, or rail-type cathode, prior to the application of the main discharge current have permitted the excitation of gas volumes with beam cross sections of ~25 cm². Systems employing this technique with output energies of ~130 J have been reported [8]. However, for reliable performance, these excitation schemes are at present limited by arcs and other instabilities to operation at input levels less than ~200 J·l⁻¹ in gas mixtures containing 10–15 percent CO_2 gas, resulting in nonsaturated gain values of ~3 percent cm⁻¹.

An alternative, though somewhat more elaborate approach employing separate volumetric preexcitation of the discharge volume by high-energy electron beams already has achieved encouraging results [13]–[17]. Daugherty has recently reported the operation of such a device having a cross-sectional area of 200 cm² and active length of 2 m, capable of generating 2000-J optical pulses of peak power of ~100 MW [15]. With this technique, energy outputs of ~50 J·l⁻¹ and gain values of ~5.0 percent cm⁻¹ are at present attainable [16]. In addition, Basov *et al.* have performed an exhaustive study of molecular gas lasers excited by means of high-current electron beams and operating at pressures considerably in excess of one atmosphere [18].

A third type of excitation scheme utilizes a discharge between Rogowski or Bruce profiled electrodes, preionization being produced by an additional discharge between a trigger electrode in the form of one or more wires that are parallel to, but laterally displaced from, the discharge axis [19]–[23]. This discharge scheme is capable of energy inputs of >400 J·l⁻¹, and streak photographs of the temporal development of the discharge indicate that UV photoemission at the cathode is the initiating mechanism, the UV radiation being presumed to result from the 584-Å He resonance line produced in the auxiliary discharge between the wire and the anode [21]. Further studies of photoemission at the cathode, using a variety of UV radiation sources and photocathode materials, have led to output energies of ~50 J·l⁻¹ for small volumes (~150 cm³) being obtained by this technique [24].

In this paper we wish to report the development of a discharge scheme that permits the efficient excitation of large volumes of CO_2, N_2, and He gas mixtures at atmospheric pressure with high CO_2 concentration (~30 percent). Preionization of the discharge volume is obtained with the aid of an auxiliary multiple spark

Manuscript received September 21, 1972. These results were first presented at the 7th International Quantum Electronics Conference, Montreal, Que., Canada, May 8–11, 1972, and subsequently at the Symposium on High Power Molecular Lasers, Laval University, Quebec, Que., Canada, May 15–17, 1972.

The authors are with the Division of Physics, National Research Council of Canada, Ottawa, Ont., Canada.

discharge from a third electrode, which is situated behind a perforated mesh anode. Time-resolved photographic studies indicate that volume photoionization of the gas by UV radiation, emitted from the multiple arcs, is the principal excitation mechanism. The onset of the main discharge between a solid cathode and the perforated anode is controlled until the optimum degree of ionization exists within the discharge volume. Thus, under these conditions, greater than 30-J·l^{-1} output energies are obtained from discharge modules having cross-sectional areas of 26 and 58 cm^2 and active volumes of 1.2 and 2.7 l, respectively. Small-signal gain measurements give an average gain of 4.3 percent cm^{-1} and indicate that peak values approaching 5 percent cm^{-1} are achieved. The overall energy extraction efficiency is >10 percent.

An initial study of this discharge scheme has been conducted to determine its performance as a beam amplifier for a high-power laser system suitable for the production of high-temperature plasmas of thermonuclear interest. When a number of these discharge modules are operated in series, in a simple oscillator configuration, total output energies of ~300 J are obtained with powers in the multigigawatt range. In addition, preliminary measurements of the optical breakdown threshold within the laser medium indicate that for beam cross sections of at least 5 cm^2, energy densities of ~20 J·cm^{-2} cannot be exceeded without the occurrence of breakdown.

II. Discharge Module and Excitation Circuit

The discharge scheme developed has been designed to permit modular construction with a view to the fabrication of large laser systems. Each set of electrodes is housed in a gas-tight Lucite box and is individually energized with its own discharge circuit. When a number of these modules are operated in series, each discharge circuit is separately triggered from a central control trigger generator. The basic arrangement of the electrode assembly is shown in Fig. 1. The main discharge occurs between a cathode consisting of a solid aluminum electrode of ~60 cm in length and 15 cm wide and an anode of similar size consisting of a fine stainless-steel mesh, tightly stretched over a Lucite or Bakelite former. Although both electrodes are flat in the central region of the discharge area, their edges are contoured to an approximately Rogowski profile [25]. In addition, the ends of the solid electrode are profiled to compensate for the nonuniform field distribution associated with the ends of the mesh electrode. The best results were obtained when the surface of the cathode had a slightly roughened character.

Initially a system having a 5-cm electrode separation was developed and subsequently scaled up to 7.5-cm separation of the same electrodes with only minor modifications. The results obtained with both systems are reported in the succeeding sections.

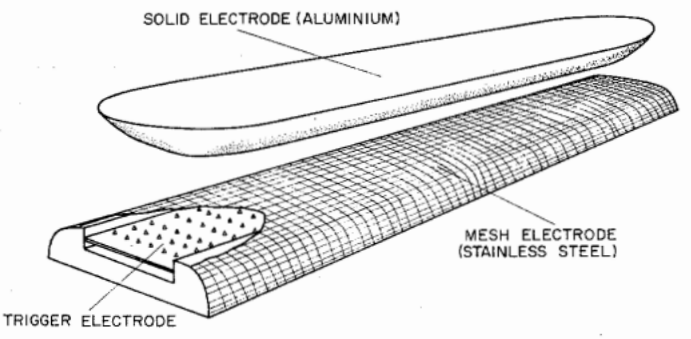

Fig. 1. Basic electrode structure of each discharge module.

The main discharge is energized by the output of a two-stage 0.2-μF capacitance Marx bank with nominal charge line voltages of 55 and 75 kV for the 5- and 7.5-cm discharge modules, respectively. The circuit is shown in Fig. 2. There are two pressurized nitrogen spark gaps SG_1 and SG_2 in the Marx circuit, one of them (SG_2) incorporating an external trigger electrode. A third pressurized spark gap (SG_3) is in series with the Marx bank and, through control of its self-triggering threshold, principally by variation of the gas pressure, determines the time after the triggering of the Marx bank at which the main current pulse occurs between the electrodes. This allows time for the preionization of the main gas volume to occur prior to the initiation of the main discharge. The preionization is facilitated by the incorporation of a third discharge electrode, the trigger electrode, (see Fig. 1) consisting of six separate strings of point electrodes, situated behind and in close proximity to the mesh electrode. Each string of electrodes consists of ~100-point electrodes and is individually capacitively coupled directly to the output of the Marx bank.

Thus the sequence of events is as follows.

1) After the second spark gap SG_2 is externally triggered, the Marx bank fires and the voltage builds up between the point electrodes and the mesh. This results initially in coronal emission from these point electrodes, providing a thin region of uniform electron gas in the vicinity of the mesh.

2) As the voltage between the point electrodes and the mesh anode continues to increase, multiple discharge arcs begin to occur in this region. These arcs provide the source of preionization of the main discharge volume.

3) After the optimum degree of preionization has been achieved, the third spark gap (SG_3) fires and the main current pulse occurs between the discharge electrodes.

The sequence and time scale of these processes will be discussed further in the following section.

The gas mixture is fed into the discharge module through simple one-way valves at flow rates up to 10 l min^{-1}. With such a flow rate the discharge has been fired at repetition rates of 10 ppm. However, no effort has been made to maximize the repetition rate, which

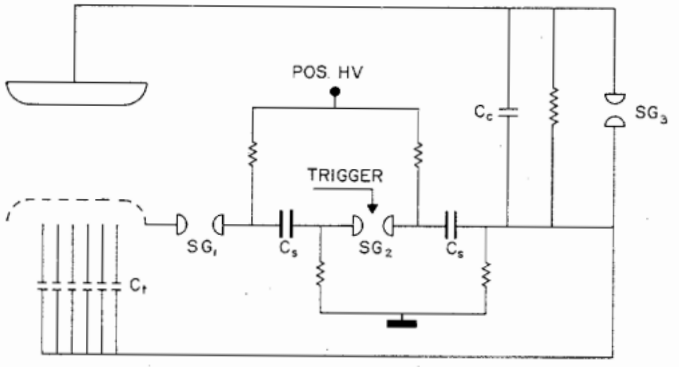

Fig. 2. Schematic of Marx bank excitation circuit. C_s—storage capacitors, 0.1 μF; C_t—trigger capacitors: C_t ~160 pF (5-cm system), C_t ~100 pF (7.5-cm system); C_c—cathode capacitor, 100 pF; SG_1, SG_2 SG_3, pressurized nitrogen spark gaps.

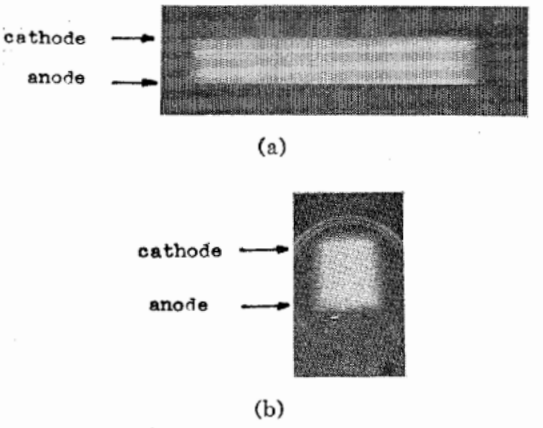

Fig. 3. Time-integrated photographs of the discharge. (a) Transverse to the electrodes. (b) Along the axis of the electrodes.

is principally limited by the capability of the charging supply.

III. Temporal Characteristics of the Discharge

Measurements of the temporal characteristics for both the 5- and 7.5-cm discharge modules have so far been restricted to observation of the discharge current waveform, and its delay relative to the Marx bank trigger pulse, a time-resolved photographic study of the preionization process, and the onset of the main discharge. In addition, time-resolved small-signal gain measurements under a variety of operating conditions will be described in a succeeding section.

Time-integrated photographs of the discharge in the 7.5-cm module are shown in Fig. 3. Fig. 3(a) shows the degree of uniformity along the length of the discharge. Although there is still some evidence of slight nonuniformity, this could probably be reduced by careful contouring of the electrodes. This photograph was obtained under the optimum gas mixture conditions (30 percent CO_2, 20 percent N_2, and 50 percent He) for an energy input of ~240 $J \cdot l^{-1}$. The system with 5-cm electrode separation was operated at somewhat higher input energies (~320 $J \cdot l^{-1}$). When energies in excess of this were discharged into the gas, small streamers emanating from the cathode for a few centimeters and occasionally completely across the discharge were observed. The 7.5-cm discharge observed along the axis is shown in Fig. 3(b). The degree of uniformity between the electrodes can clearly be seen. In addition, below the mesh anode it is possible to observe the small arcs between the point electrodes and the mesh that give rise to preionization of the main gas volume between the anode and the cathode.

Time-resolved studies of this projection of the discharge were undertaken in order to determine the history of the discharge and to ascertain more clearly the sequence and effect of the preionization system. An image of the central region of the discharge was focused onto the S1 photocathode of a TRW image-converter camera operating in the streaking mode and time-resolved photographs of the discharge obtained under a variety of operating conditions. In addition, the discharge current waveform was simultaneously monitored with the aid of an integrating Rogowski coil of the type developed by Pellinen and Spence [26], which recorded the current passing through the spark gap SG_3. A typical result, recorded under optimum operating conditions for the 7.5-cm discharge, is shown in Fig. 4.

The sequence of events, as already outlined in the last section, can clearly be seen. Initially, coronal discharges occur between the point electrodes and the mesh anode. This coincides with the initial sharp spike recorded by the current monitoring device. After some 50–60 ns, the luminosity in this region suddenly increases as multiple arcs form due to the rapidly rising voltage applied to these electrodes. Concurrent with the occurrence of these arc discharges, the volume of the gas between the mesh electrode and cathode is partially ionized, as can be seen from the region of weak illumination in the streak photograph. It should be noted that the onset of this ionization is extremely fast, less than 10 ns, and also that it extends almost completely across the anode–cathode region but is most intense nearest the anode and the multiple arcs. Such a phenomenon cannot be explained by the propagation of electrons originating in the region between the trigger electrode and the anode. Thus, time-resolved photography of the discharge appears to confirm the hypothesis that the rapid onset of partial ionization of the gas is caused by short-wavelength UV radiation emanating from the multiple arcs formed between the point electrodes and the mesh. However, the effects of other processes, such as those associated with the production of a weak electron gas in the vicinity of the anode and the effectiveness of UV photoemission at the cathode, may also be playing some role in maintaining a uniform discharge. The presence of a uniform distribution of electrons around the mesh electrode may have the effect of producing a smoother electrode than that of the wire mesh alone. Although the effect of photoemission from the aluminum cathode cannot at present

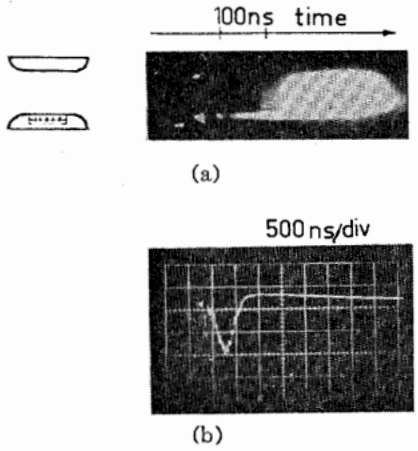

Fig. 4. Discharge development and discharge current waveform under optimum operating conditions for an electrode separation of 7.5 cm. Gas mixture—30 percent CO_2, 20 percent N_2, 50 percent He. Input energy—240 J · l^{-1}. (a) isolated bright spots unfortunately result from a defect within the image converter tube caused by electron noise generated near the photocathode and are not associated with the recorded image of the discharge. (b) Signal recorded by the integrating Rogowski coil.

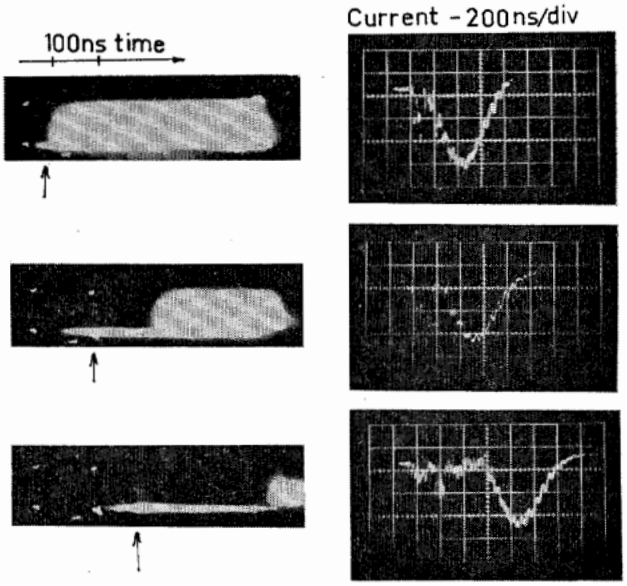

Fig. 5. Discharge obtained under conditions of variable delay between preionization of the discharge volume (as per arrow) and the occurrence of the main discharge. The current pulse waveform is also shown.

be determined, the requirement of a low-impedance path in the cathode circuit during the preionization stage indicates the existence of some cathodic effects.

Following the production of this degree of ionization, the spark gap SG_3 spontaneously fires, and the main discharge current flows between the anode and the cathode. This is shown in the streak photograph by the onset of the region of increased luminosity, and the Rogowski probe registers the smoothly varying waveform of the main discharge current. It can be seen, and is more evident on streak photographs of less exposure, that the maximum luminosity of the main discharge occurs closest to the anode where the greatest degree of ionization would be expected if volumetric photoionization of the gas were the initiating process. This should be contrasted with the time-resolved studies of the system devised by Lamberton and Pearson [19], [21]. These show the greatest degree of illumination of the main discharge occurring nearest the cathode, consistent with their hypothesis of UV photoexcitation at the cathode surface being the dominant mechanism.

The degree to which the initiation of the main discharge may be delayed relative to the onset of initial preionization by variation of the over-voltage requirements of the spark gap SG_3 is demonstrated in Fig. 5. These three streak photographs and their accompanying current waveforms were obtained under reduced input energy conditions (~180 J·l^{-1}) with the spark gap SG_3 adjusted to fire at different times after the initiation of the preionization. It can be seen that the main discharge can be delayed by as much as 400 ns after the initial volumetric preionization is produced. In particular the lower streak photograph shows the onset of the main discharge occurring at a time when the preionization discharge between the point electrodes and the mesh has almost lapsed. In this case, and in the center photograph, the weak illumination resulting from the preionization can be distinguished and it can be seen that although this illumination decays, conditions within the active region are still sufficient to sustain the main discharge after ~400 ns. However, for longer delay times between the preionization and the onset of the main discharge, the maximum permissible input energy, without the formation of arcs, is reduced.

IV. Small-Signal Gain Measurements

Measurements of the small-signal gain were made on a single discharge module having an electrode separation of 5 cm. A nominal 30-W continuous output CO_2 laser having a single line emission $P(16)$ was used in these studies, the discharge module being situated some 5 m from the output of the CW laser and an aperture of 5 mm diameter used to limit the size of the beam. The single pass transmitted beam was recorded with an HgTe:CdTe detector and an oscilloscope, and the dependence of the small-signal gain on gas mixture composition and energy input was obtained. In addition, the spatial gain profile between the electrodes was investigated.

A typical oscilloscope trace of the recorded gain signal is shown in Fig. 6. The two spots at the beginning of the trace show the amplitude of the dc signal level from the CW CO_2 laser. As can be seen, the rise time of the gain pulse is less than 1 μs and the decay time ~5 μs. It was found in these studies that the duration of the gain pulse was a function of the maximum gain, and in the results that follow, the duration (HPPW) of the gain pulse is also plotted as a function of the various parameters of gas, energy, and spatial position.

Fig. 7(a) shows the variation of the small signal gain

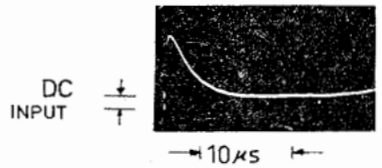

Fig. 6. Oscilloscope trace of recorded gain signal showing dc input power level.

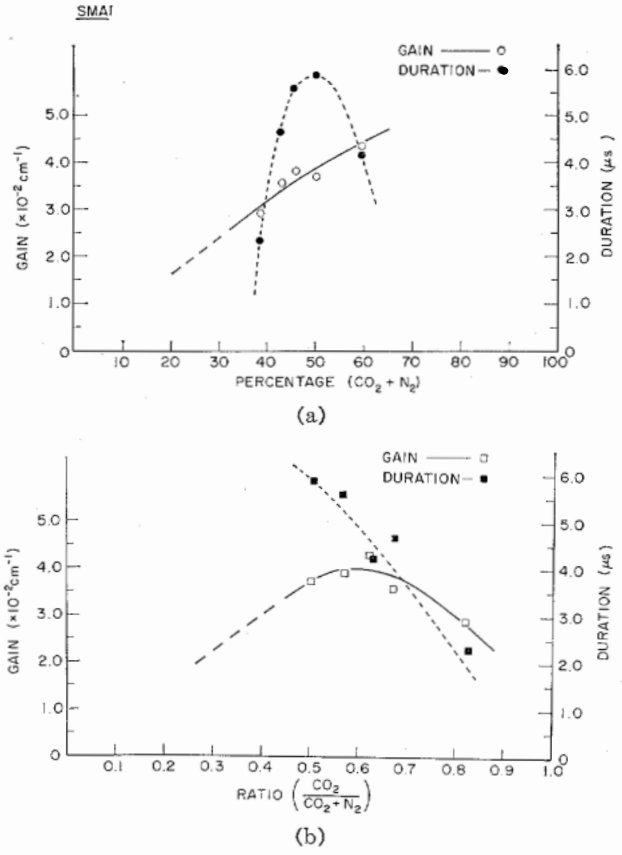

Fig. 7. Variation of small-signal gain as a function of gas composition for fixed energy input of 260 J·l⁻¹. (a) As a function of percentile CO_2 and N_2 gas. (b) As a function of ratio of CO_2 to N_2 for He concentration of ~50 percent.

as a function of the percentile CO_2 and N_2 gas in the discharge volume for an input energy of 260 J·l^{-1}, the ratio of CO_2 to N_2 remaining in the range 1–2. It can be seen that the gain progressively increases as the ratio of CO_2 and N_2 is increased, maximum values in the center of the discharge of ~4.3 percent cm^{-1} being obtained at a (CO_2 + N_2) gas composition approaching 60 percent. At higher CO_2 concentrations, the output from the discharge module becomes irreproducible, and there is a tendency for arc discharges to form. Fig. 7(b), which shows the gain as a function of relative CO_2 to N_2 concentration, indicates an optimum ratio of CO_2 to N_2 of 3:2 for maximum gain.

The variation of the gain as a function of energy input per unit volume is shown in Fig. 8, and appears to indicate that maximum gain values are obtained at input energies of ~260 J·l^{-1}. However, the input energy

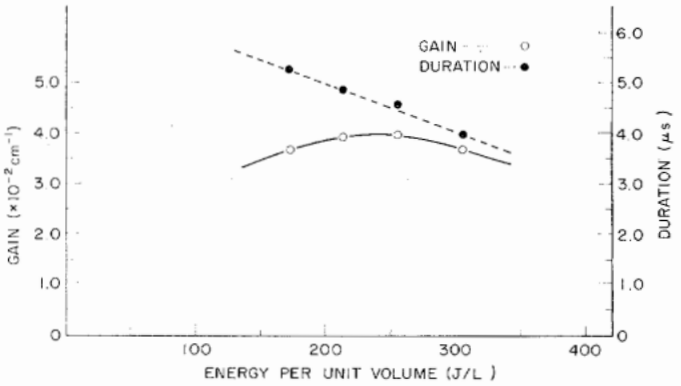

Fig. 8. Variation of small-signal gain as a function of input energy per unit volume (26 percent CO_2, 54 percent He, and 20 percent N_2).

was varied by changing the Marx-bank charge line voltage, and hence also the E/p values of both the main discharge and the preionization discharges.

To obtain the small signal gain profile between the electrodes, the 5-mm-diameter CW CO_2 laser beam was traversed across the discharge and measurements of the gain were made at different points between anode and cathode. The resulting variation of the gain is shown in Fig. 9. As can be seen the gain profile is fairly flat in the central region of the discharge but increases toward the anode and decreases almost to a corresponding degree on the cathode side. However, in the construction of a laser-beam amplifier utilizing several discharge modules, the effect of this nonuniformity of the gain profile near the electrodes can largely be eliminated by alternating the orientation of adjacent discharge modules such that the edge of the amplified beam would run through cathode and anode regions alternately. Thus, the overall gain would be fairly well matched across the whole discharge.

V. Characteristics of a High-Power High-Energy Laser Oscillator

In order to demonstrate that significant powers and high-energy extraction efficiencies can be obtained with the discharge modules described in the preceding sections, seven such modules were operated in series in a simple laser oscillator configuration. Initially the system employed an electrode separation of 5 cm but more recent results have been obtained with an electrode spacing of 7.5 cm. The laser system and diagnostic techniques used to investigate the beam are shown schematically in Fig. 10.

The optical resonator of the laser was formed by a plane fully reflecting Au mirror M and a single NaCl flat S_M. The individual discharge modules were alternated in position, as discussed in the preceding section. The Marx bank for each module was charged from a central power supply, and the triggered pressurized spark gap of each bank simultaneously switched from a common trigger source. Gas was fed to each module by

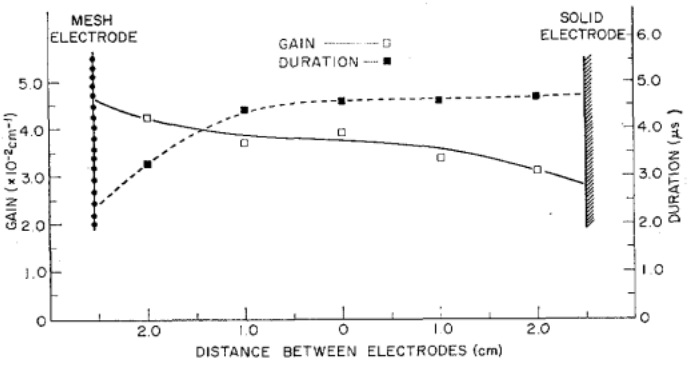

Fig. 9. Small-signal gain profile between discharge electrodes for fixed input energy density of 260 J·l⁻¹ and gas composition of 26 percent CO_2, 54 percent He, and 20 percent N_2.

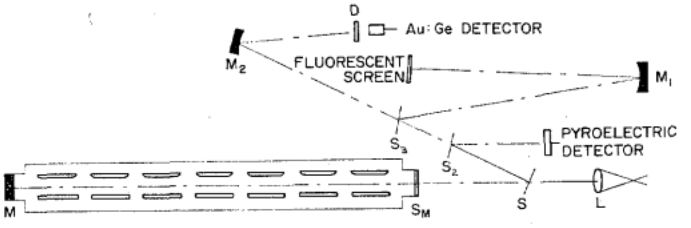

Fig. 10. Schematic of experimental arrangement of seven-module laser oscillator. M—plane fully reflecting Au mirror. S_M—uncoated NaCl mirror. M_1, M_2—concave Au mirrors of radius of curvature 5 and 6 m, respectively. S_1, S_2, S_3—NaCl flats. D—NaCl diffuser. L—NaCl lens.

equal lines from a common gas mixing system. The whole assembly was mounted inside a grounded copper mesh enclosure to reduce the effects of electrical noise on diagnostic equipment.

Measurement of the laser output was made by sampling the beam with a single NaCl flat S_1 and utilizing a pyroelectric detector of the type developed by Lachambre [27], which was illuminated by the reflected beam from a second NaCl flat S_2. The pyroelectric detector was calibrated in the same energy range in which it was used (1–5 J) by cross reference with the output of a solid-state laser, which itself was monitored with a calibrated thermopile. The calibration of the pyroelectric detector was also compared with that of a commercially available device,[1] and agreement was within 20 percent.

The temporal development of the laser pulse was monitored by partially focusing the sample beam from S_1 with mirror M_2 onto an NaCl diffuser D, detection being made with a fast (nominally 1-ns rise time) Au-doped Ge detector. The signal from the latter was displayed on a 519 oscilloscope after passage through a 35-dB-gain 2-ns-rise-time pulse amplifier. Typical pulse shapes of the laser output are shown in Fig. 11. As can be seen, with the optimum gas mixture the output consists of an initial 10-ns-rise-time pulse of ~50-ns duration, followed by a low-intensity tail of ~1-μs duration.

[1] Gen-Tec pyroelectric detector-type ED-200.

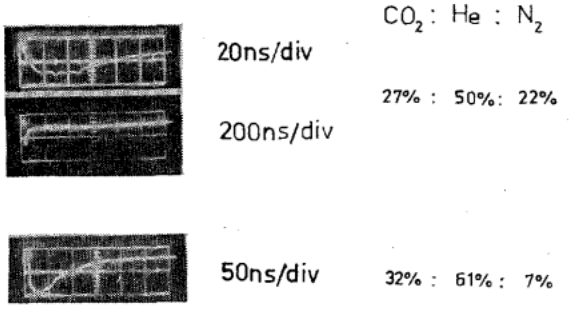

Fig. 11. Typical temporal waveforms of the laser beam output.

When the discharge is operated with low N_2 concentration, this tail is almost eliminated.

Brightness measurements were made with a fraction of the sample beam reflected off an NaCl flat S_3, and focused with a 3-m focal-length mirror onto an infrared thermal image plate. Photography of the resulting beam pattern indicated a beam divergence of ~2 mrad.

The principal output characteristics of the laser system for electrode separations of 5 and 7.5 cm are summarized in Table I. It should be noted that several factors at present limit the performance of the system with 7.5-cm electrode spacing. Principal among these is a limitation to 75-kV charging voltage on the Marx bank. Thus, the input energy is restricted to ~210 J·l⁻¹ and also somewhat lower E/p values than those that were required for optimum performance of the 5-cm system. When operated at maximum output, the energy density within the 5-cm system is ~8.5 J·cm⁻². Although this resulted in the NaCl laser mirrors having a limited life, it was found that the type of deterioration of the mirrors fell into one of two categories. A small number of NaCl flats that were used as laser mirrors experienced severe damage within a few laser shots, the damage being extensive and symptomatic of the NaCl having

TABLE I
PRINCIPAL CHARACTERISTICS OF THE NRC CO_2 LASER

	5-cm System	7.5-cm System
Number of discharge modules	7	7
Total active volume	8.4 l	18.9 l
Active cross-sectional area	25.8 cm²	58.1 cm²
Optical resonator length	5.8 m	6.8 m
Operating voltage (nominal)	55 kV	75 kV
Total input energy (nominal)	2100 J	3900 J
Optimum gas composition	30 percent CO_2; 20 percent N_2 50 percent He;	30 percent CO_2 20 percent N_2 50 percent He
Conversion efficiency	~10 percent	~8 percent
Average gain	~4.3 percent /cm	—
Maximum output energy	220 J	~300 J
Maximum output power	>2 GW	>3 GW
Pulse duration (initial)	50 ns	50 ns
(tail)	1–2 μs	1–2 μs
Brightness	>3 10^{13} W·cm⁻²·sr⁻¹	—

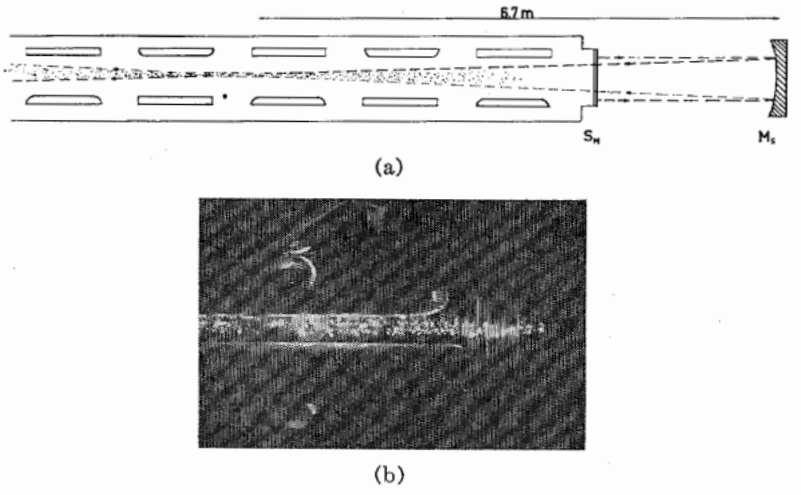

Fig. 12. (a) Experimental setup for the determination of the optical breakdown threshold within the laser medium. (b) Character of optical breakdown within one of the discharge modules. Electrode separation 5 cm.

contained inclusions of some type. However, the damage to most of the NaCl flats used was less violent in character, and principally consisted of the progressive appearance (after several hundred shots) of small hairline cracks in the polished surface along natural cleavage planes of the crystal.

VI. Optical Breakdown Within the Laser Medium

As is the case in the construction of all high-power laser systems, the ultimate limitation on the power density that can be sustained within the laser is that at which optical breakdown of the laser medium occurs. It is interesting to consider this problem for the case of high-power CO_2 lasers, especially in the light of recent experiments on focused 10.6-μ radiation optical breakdown of gases [28], [29], which show that as the focal-spot diameter is increased from $\sim$100 μ, the threshold energy density required for optical breakdown decreases until, in the region of 0.1–0.2 cm, the threshold appears to level off to a minimum value ($\sim$10 J·cm^{-2} for a 70-ns laser pulse in CO_2 laser gas at atmopheric pressure [30]). Since for these experiments, the focal-spot size was much greater than the calculated electron diffusion distance, this dependence on focal diameter cannot be explained on the basis of electron diffusion losses. Although Smith has suggested the possible existence of a loss mechanism depending on atomic excitation resonance radiation trapping [28], [30], an alternative explanation, depending upon the existence within the the focal volume of particulate matter large enough to ignite a self-sustaining plasma, has been proposed [29], [31].

In view of these results, a better understanding of the processes governing the optical breakdown of active-laser gas mixtures is particularly relevant to the construction of large laser systems [31]–[33]. It is interesting to note that in the laser system with 5-cm electrode separation, the energy density within the beam is 8.5 J·cm^{-2} ($\sim$6 J·cm^{-2} in the first short 50-ns pulse) and no optical breakdown was observed. Thus, a simple experiment was performed to obtain an estimate of the radiation flux required for optical breakdown within the laser medium for large apertures. The output of the 5-cm system was focused by a long-focal-length mirror (6.7-m focal length) back into the laser medium as shown in Fig. 12(a). Breakdown points were observed to occur for a distance of $\sim$2.9 m on either side of the focal point, when the laser energy was reduced to the 100–120 J range. Fig. 12(b) is typical of the random character of the breakdown points within one of the discharge modules. By determining the power density at that point farthest from the focus at which optical breakdown occurred, an estimate of the breakdown threshold within the laser medium could be made. Thus it was found that energy densities below $\sim$20 J·cm^{-2} (13 J·cm^{-2} in the first 50 ns) over cross-sectional areas of 5 cm^2 were insufficient for the spontaneous occurrence of optical breakdown in the medium (30 percent CO_2, 20 percent N_2, and 50 percent He).

VII. Conclusions

Although many unanswered questions remain, several comments may be made on the discharge scheme described previously. Its development has demonstrated that a large aperture TEA laser module may be constructed with high input energies (>300 J·l^{-1}) into 30 percent CO_2, He and N_2 gas mixtures, resulting in high optical gain (>4 percent cm^{-1}) and >10 percent energy extraction efficiency over beam cross-sectional areas up to 60 cm^2. This has been achieved with the aid of a sheet of small arc discharges, initiated prior to the occurrence of the main discharge, and situated parallel to and in close proximity behind one of the electrodes. Undoubtedly, further study of volumetric preionization by UV radiation is required, and this hopefully will lead to the efficient excitation of larger volumes of gas with beam cross section exceeding those quoted here. In addition, it could also make possible the employment

of lower E/p values than those used in this device. The E/p values of ~20 kV cm^{-1} atm^{-1} utilized in the present system primarily result from the necessity of having a very high voltage trigger source and the employment of a single-discharge circuit to accomplish both preionization and driving of the main discharge. Finally, by employing several discharge modules in series in a simple laser oscillator configuration, output pulses with energies of ~300 J and powers in the multigigawatt range have been generated.

In the construction of larger high-power high-energy systems, the need to employ greater beam apertures is vividly demonstrated when it is realized that the 5-cm system described here, capable of a maximum energy output of 220 J, operates at a power density within ~40 percent of that required for optical breakdown of the medium. In addition, the use of a number of discharge modules as a beam amplifier, perhaps for short nanosecond or subnanosecond pulses generated by mode-locking or other techniques, will require effective means of optical isolation of the amplifier units. The solution of these problems should permit the construction of CO_2 laser systems generating short pulse outputs in the multikilojoule range.

Acknowledgment

The authors wish to thank Dr. T. Oka of the Physics Division for use of his CW CO_2 laser and J. N. Cairns of the Physics Division Optical Workshop for an unfailing supply of fresh NaCl flats. The participation of other members of the Laser and Plasma Physics Group of NRC is also acknowledged, especially that of W. Orr, whose electronics expertise was invaluable during the course of this project.

References

[1] C. Frapard, M. Roulot, and X. Ziegler, "High peak power pulsed 10 μ CO_2 laser," *Phys. Lett.*, vol. 20, p. 384, 1966.
[2] A. E. Hill, "Multijoule pulses from CO_2 lasers," *Appl. Phys. Lett.*, vol. 12, p. 324, 1968.
[3] G. J. Dezenberg, E. L. Roy, and W. B. McKnight, "Performance of high-voltage axially pulsed CO_2 lasers," *IEEE J. Quantum Electron.*, vol. QE-8, p. 58–65, Feb. 1972.
[4] D. A. Leonard, "Saturation of the molecular nitrogen second positive laser transition," *Appl. Phys. Lett.*, vol. 7, p. 4, 1965.
[5] R. Dumanchin and J. Rocca-Serra, "Augmentation de l'énergie et de la puissance fournies par unité de volume dans un laser à CO_2 en régime pulsé," *C. R. Acad. Sci.* (Paris), vol. 269B, p. 916, 1969.
[6] A. J. Beaulieu, "Transversely excited atmospheric pressure CO_2 lasers," *Appl. Phys. Lett.*, vol. 16, p. 504, 1970.
[7] A. K. Laflamme, "Double discharge excitation for atmospheric pressure CO_2 lasers," *Rev. Sci. Instr.*, vol. 41, p. 1578, 1970.
[8] R. Dumanchin, J. C. Farcy, M. Michon, and J. Rocca-Serra, "High power density pulsed molecular laser," presented at the 6th Int. Quantum Electronics Conf., Kyoto, Japan, 1970.
[9] R. Dumanchin, M. Michon, J. C. Farcy, G. Boudinet, and J. Rocca-Serra, "Extension of TEA CO_2 laser capabilities," *IEEE J. Quantum Electron.*, vol. QE-8, pp. 163–165, Feb. 1972.
[10] Y.-L. Pan, A. F. Bernhardt, and J. R. Simpson, "Construction and operation of a double-discharge TEA CO_2 laser," *Rev. Sci. Instr.*, vol. 43, p. 662, 1972.
[11] R. Fortin, A. K. Laflamme, and F. Rheault, "Double-discharge TEA laser beams," *Can. J. Phys.*, vol. 50, p. 583, 1972.
[12] P. E. Dyer, D. J. James, and S. A. Ramsden, "Single transverse mode operation of a pulsed volume excited atmospheric pressure CO_2 laser using an unstable resonator," *Opt. Commun.*, vol. 5, p. 236, 1972.
[13] C. A. Fenstermacher, M. J. Nutter, W. T. Leland, and K. Boyer, "Electron-beam-controlled electrical discharge as a method of pumping large volumes of CO_2 laser media at high pressure," *Appl. Phys. Lett.*, vol. 20, p. 56, 1972.
[14] R. K. Garnsworthy, L. E. S. Mathias, and C. H. H. Carmichael, "Atmospheric-pressure pulsed CO_2 laser utilizing preionization by high energy electrons," *Appl. Phys. Lett.*, vol. 19, p. 506, 1971.
[15] J. D. Daugherty, "Electron-beam sustainer CO_2 lasers," presented at the 7th Int. Quantum Electronics Conf., Montreal, Que., 1972.
[16] C. A. Fenstermacher, W. T. Leland, M. J. Nutter, and J. P. Rink, "Parametric studies of the electron beam controlled discharge in CO_2 laser media," presented at the 7th Int. Quantum Electronics Conf., Montreal, Canada, 1972.
[17] N. G. Basov, E. M. Belenov, V. A. Danilychev, and A. F. Suchkov, "High pressure pulsed CO_2 laser," *Kvantovaya Electron.*, vol. 3, p. 121, 1971; also *Sov. J. Quantum Electron.*, vol. 1, p. 306, 1971.
[18] N. G. Basov, "Electroionization lasers," presented at the 7th Int. Quantum Electronics Conf., Montreal, Canada, 1972.
[19] H. M. Lamberton and P. R. Pearson, "Improved excitation techniques for atmospheric pressure CO_2 lasers," *Electron. Lett.*, vol. 7, p. 141, 1971.
[20] A. Crocker and H. M. Lamberton, "Output pulse characteristics and self-mode locking of atmospheric pressure CO_2 lasers," *Electron. Lett.*, vol. 7, p. 272, 1971.
[21] P. R. Pearson and H. M. Lamberton, "Atmospheric pressure CO_2 lasers giving high output energy per unit volume," *IEEE J. Quantum Electron.*, QE-8, pp. 145–149, Feb. 1972.
[22] L. J. Denes and O. Farish, "High pressure pulsed carbon dioxide laser with uniform excitation," *Electron. Lett.*, vol. 7, p. 337, 1971.
[23] T. Y. Chang and O. R. Wood, "A simple self-mode locked atmospheric pressure CO_2 laser," *IEEE J. Quantum Electron.* (Corresp.), vol. QE-8, pp. 721–723, Aug. 1972.
[24] H. J. J. Sequin and J. Tulip, "High energy high power TEA CO_2 laser using a photocathode," presented at the 7th Int. Quantum Electronics Conf., Montreal, Canada, 1972.
[25] J. D. Cobine, *Gaseous Conductors—Theory and Engineering Applications*. New York: McGraw-Hill, 1941, ch. 7.
[26] D. G. Pellinen and P. W. Spence, "Nanosecond risetime megampere current monitor," *Rev. Sci. Instr.*, vol. 42, p. 1699, 1971.
[27] J. L. Lachambre, "A pyroelectric energy meter," *Rev. Sci. Instr.*, vol. 42, p. 74, 1971.
[28] D. C. Smith, "Gas breakdown dependence on beam size and pulse duration with 10.6 μ wavelength radiation," *Appl. Phys. Lett.*, vol. 19, p. 405, 1971.
[29] L. C. Marquet, R. J. Hull, and D. E. Lencioni, "Studies of breakdown in air by a pulsed CO_2 laser," presented at the 7th Int. Quantum Electronics Conf., Montreal, Canada, 1972.
[30] P. J. Berger and D. C. Smith, "Gas breakdown in the laser as the limitation of pulsed high pressure CO_2 lasers," *Appl. Phys. Lett.*, vol. 21, p. 171, 1972.
[31] G. H. Canavan, W. A. Proctor, P. E. Neilsen, and S. D. Rockwood, "CO_2 laser air breakdown calculations," presented at the 7th Int. Quantum Electronics Conf., Montreal, Canada, 1972.
[32] S. D. Rockwood, G. H. Canavan, and W. A. Proctor, "Gas breakdown within the cavity of CO and CO_2 lasers and amplifiers," presented at the 3rd Conf. Chemical and Molecular Lasers, St. Louis, Mo., 1972.
[33] Yu. V. Afanas'ev, E. M. Belenov, and I. A. Poluektov, "Optical breakdown of molecular gases," *JETP Lett.*, vol. 15, p. 41, 1972.